Characterization of Polymer Solutions Containing a Small Amount of Aggregates by Static and Dynamic Light Scattering

Masaaki Kanao, Yasuhiro Matsuda, and Takahiro Sato*,†

Department of Macromolecular Science, Osaka University, 1-1 Machikaneyama-cho, Toyonaka, Osaka 560-0043, Japan

Received August 26, 2002; Revised Manuscript Received December 17, 2002

ABSTRACT: Aggregate-containing solutions of poly(*n*-hexyl isocyanate) (PHIC) and atactic polystyrene of finite concentrations were studied by static and dynamic light scattering. Their static structure factors $\hat{S}(k)$ and the intensity autocorrelation functions $g^{(2)}(t)$ exhibited the enhanced low-angle scattering and bimodal relaxation, respectively. From $\hat{S}(k)$ and $g^{(2)}(t)$ obtained, the fast- and slow-mode components of the static structure factor ($\hat{S}_{fast}(k)$ and $\hat{S}_{slow}(k)$) and of the first cumulant (Γ_{fast} and Γ_{slow}) were estimated as functions of the magnitude of the scattering vector k. As verified by a theory based on the dynamic mean-field theory, if the solution contains only a small amount of aggregates with diffusion coefficients much smaller than that of the nonaggregating component, $\hat{S}_{fast}(k)$ and Γ_{fast} give us the osmotic compressibility $\partial c/\partial\Pi$ and mutual diffusion coefficient D_m of aggregate-free solutions, respectively, and $\hat{S}_{slow}(k)$ and Γ_{slow} provide us the radius of gyration $\langle S^2\rangle_{z,A}^{1/2}$ and hydrodynamic radius $R_{H,A}$ of aggregates, respectively, even at a finite polymer concentration, in a good approximation. In fact, the results of $\partial c/\partial\Pi$ and D_m obtained were favorably compared with theories for binary polymer solutions without aggregates. For PHIC solutions, aggregates of lower molecular weight samples had larger $\langle S^2\rangle_{z,A}^{1/2}$ and $R_{H,A}$, indicating that the aggregates of lower molecular weight PHIC consist of a larger number of polymer chains. Furthermore, the ratio of $\langle S^2\rangle_{z,A}^{1/2}$ to $R_{H,A}$ indicated that aggregates of higher-molecular-weight PHIC are rigid-chain-like but those of lower-molecular-weight PHIC are spherelike.

Introduction

The aggregation in polymer solutions often hinders from characterizing polymer molecules and solution properties (e.g., thermodynamic and spatial properties and mutual diffusion coefficients) by static and dynamic light scattering. Thus, so far, many efforts have been made to eliminate polymer aggregates from test solutions of light scattering measurements. However, in some polymer solutions, especially with high polymer concentration or poor solubility, the aggregation is inevitable, which makes the characterization of those solutions by light scattering difficult.

In recent years, on the other hand, the characterization of polymer aggregates themselves has attracted considerable attention, mainly due to their industrial and pharmaceutical applications.[1,2] Since light scattering is very sensitive to a tiny amount of larger particles in solution, it can be used as a tool for detecting polymer aggregates in test solutions. However, quantitative characterization of aggregates by light scattering involves the following problems. The aggregation often takes place in a polymer solution of a finite concentration, where the aggregating component interacts with the nonaggregating one. In general, this interaction makes it difficult to extract the radius of gyration or hydrodynamic radius of aggregates from light scattering data. Although this interaction effect can be eliminated by extrapolating the data to the zero polymer concentration, this procedure is not available if the degree of aggregation depends on the concentration. Moreover, aggregates formed in polymer solutions are usually polydisperse, and the polydispersity correction is necessary to the radius of gyration or hydrodynamic radius, even if they are obtained.

† Also at CREST, Japan Science and Technology.

In the present study, we have first formulated the dynamic structure factor of a multicomponent polymer solution with a finite polymer concentration on the basis of the dynamic mean-field theory originally developed by Doi et al.[3] The theoretical result has demonstrated that even at a finite total polymer concentration, light scattering data can yield the radius of gyration $\langle S^2\rangle_{z,A}^{1/2}$ and hydrodynamic radius $R_{H,A}$ of the aggregating component in a good approximation, if the aggregating component is much larger than the nonaggregating one and its amount is small enough. Moreover, the theory has proposed a method for extracting the static and dynamic structure factors of the aggregate-free solution from light scattering data of aggregate-containing polymer solutions.

Taking advantage of these theoretical results, we have estimated $\langle S^2\rangle_{z,A}^{1/2}$ and $R_{H,A}$ of the aggregating component as well as the osmotic compressibility $\partial c/\partial\Pi$ and the mutual diffusion coefficient D_m of aggregate-free solutions, from static and dynamic light scattering data of quenched *n*-hexane solutions of poly(*n*-hexyl isocyanate) (PHIC) and of a concentrated tetrahydrofuran (THF) solution of atactic polystyrene containing a small amount of aggregates. Here PHIC and polystyrene were chosen as typical examples of stiff and flexible polymers, respectively. We have further argued the conformation of the polymer aggregates from the ratio of $\langle S^2\rangle_{z,A}^{1/2}$ to $R_{H,A}$ after making the polydispersity correction using the relaxation spectrum of the intensity autocorrelation function, while comparing $\partial c/\partial\Pi$ and D_m of aggregate-free solutions with theories for binary polymer solutions.

Theoretical Section

Dynamic Mean-Field Theory. Let us consider a multicomponent polymer solution containing the molecularly dispersed polymer (species 1) and its ag-

10.1021/ma0213899 CCC: $25.00
Published on Web 02/28/2003

gregates (species $2 - r$). We assume that species 1 is monodisperse, and the aggregation does not modify the polarizability of monomer units which the polymer chain consists of. The translational motion of species s ($s = 1 - r$) can be expressed in terms of the single-particle distribution function $f_s(\mathbf{r};t)$ at a time t, where $\mathbf{r}$ is the coordinates of the center-of-mass position of the polymer or aggregate in solution. The kinetic equation for $f_s(\mathbf{r};t)$ at a finite concentration may be written as[3,4]

$$\frac{\partial f_s}{\partial t} = D_s \nabla_{\mathbf{r}} \cdot [\nabla_{\mathbf{r}} f_s + f_s \nabla_{\mathbf{r}} (h_s + W_s)] \quad (s = 1 - r) \quad (1)$$

where D_s is the self-diffusion coefficient of species s, $\nabla_{\mathbf{r}}$ is the gradient operator in the three-dimensional space, and h_s and W_s are respectively the potentials of external field and of the molecular field created by surrounding polymer and aggregates, depending on $\mathbf{r}$ of species s.

In a mean-field approximation, W_s is calculated from an effective interaction potential $w_{su}(\mathbf{r} - \mathbf{r}')$ between two species s and u located at $\mathbf{r}$ and $\mathbf{r}'$, respectively, by

$$W_s = \sum_{u=1}^{r} \int \mathrm{d}\mathbf{r}'\, w_{su}(\mathbf{r} - \mathbf{r}') c'_u f_u(\mathbf{r}';t) \quad (2)$$

where c'_u is the number concentration of species u in the solution. Applying the smoothed-density theory for the second virial coefficient,[5] we may write $w_{su}(\mathbf{r} - \mathbf{r}')$ as

$$w_{su}(\mathbf{r} - \mathbf{r}') = \beta_{su} \int \mathrm{d}\mathbf{R} \int \mathrm{d}\mathbf{b} \int \mathrm{d}\mathbf{b}'\, \rho_s(\mathbf{b})\, \rho_u(\mathbf{b}')\, \delta[\mathbf{R} - (\mathbf{r} + \mathbf{b})]\, \delta[\mathbf{R} - (\mathbf{r}' + \mathbf{b}')] \quad (3)$$

Here β_{su} is the (effective) strength of interaction between two monomer units belonging to species s and u, $\rho_s(\mathbf{b})$ is the average monomer-unit density of species s at the position separated by $\mathbf{b}$ from its center of mass, $\delta(\mathbf{x})$ is the delta function, and the integration with respect to a vector $\mathbf{R}$ is carried out over the whole volume V of the solution.

To formulate the dynamic structure factor $\hat{S}(k,t)$, Doi et al.[3] introduced a fictitious time-dependent external field by which species s feels the potential

$$h_s = -\xi_s(t) N_{0,s} s_{\mathbf{k},s} \mathrm{e}^{-i\mathbf{k}\cdot\mathbf{r}} \quad (4)$$

where $\mathbf{k}$ is the scattering vector, $\xi_s(t)$ is the perturbation parameter, $N_{0,s}$ is the number of monomer units which species s consists of, and $N_{0,s} s_{\mathbf{k},s}$ is the Fourier transform of the monomer-unit density $\rho_s(\mathbf{b})$: $N_{0,1}$ is the degree of polymerization of the polymer chain (species 1), and $s_{\mathbf{k},s}$ tends to unity at $k \to 0$. By the perturbation h_s, the distribution function deviates from the thermally equilibrium value by $f_{\mathbf{k},s}(t)$, which is calculated from the following equation:

$$\frac{\partial}{\partial t} f_{\mathbf{k},s}(t) = -\Gamma_{s1} f_{\mathbf{k},1}(t) - \Gamma_{s2} f_{\mathbf{k},2}(t) \ldots - \Gamma_{sr} f_{\mathbf{k},r}(t) + \xi_s(t) N_{0,s} D_s k^2 s_{\mathbf{k},s} \quad (5)$$

($s = 1 - r$), where Γ_{su} is defined by

$$\Gamma_{su} = D_s k^2 (\delta_{su} + c'_u w_{\mathbf{k},su}) \quad (6)$$

with the Kronecker's delta δ_{su} and the Fourier transform $w_{\mathbf{k},su}$ of $w_{su}(\mathbf{r} - \mathbf{r}')$. Using the apparent second virial coefficient γ_{su} ($\equiv \beta_{su} N_A / 2 M_0^2$; N_A, the Avogadro constant; M_0, the molar mass of the monomer unit common to all the components) between species s and u at the finite concentration, eq 6 can be rewritten as

$$\Gamma_{su} = D_s k^2 (\delta_{su} + 2 w_u M_0 N_{0,s} s_{\mathbf{k},s} s_{\mathbf{k},u} \gamma_{su} c) \quad (7)$$

where w_u is the weight fraction of species u in the total polymer and c is the total mass concentration of polymer and aggregates in the solution. The quantities γ_{su} may depend on s, u, and concentrations of all species.[6]

For the weak perturbation, the general solution of eq 5 can be written in the form

$$f_{\mathbf{k},s}(t) = (V c'_s N_{0,s} s_{\mathbf{k},s})^{-1} \sum_{u=1}^{r} \int_{-\infty}^{t} \chi_{\mathbf{k},su}(t - t')\, \xi_u(t')\, \mathrm{d}t' \quad (8)$$

and from the fluctuation−dissipation theorem the response function $\chi_{\mathbf{k},su}$ in eq 8 is related to the partial dynamic structure factor $\hat{S}_{su}(k,t)$ ($1 \le s, u \le r$) by

$$\hat{S}_{su}(k,t) = (V \sum_{v=1}^{r} c'_v N_{0,v})^{-1} \int_t^{\infty} \chi_{\mathbf{k},su}(t')\, \mathrm{d}t' \quad (9)$$

The total dynamic structure factor $\hat{S}(k,t)$ is given by

$$\hat{S}(k,t) = \sum_{s,u=1}^{r} \hat{S}_{su}(k,t) \quad (10)$$

where we have assumed equal scattering power of the monomer unit of all the components.

Approximation. To obtain the explicit functional form of $\chi_{\mathbf{k},su}$, we have to solve the simultaneous differential equations 5 ($s = 1 - r$). If the solution contains only a small amount of aggregates, interactions among aggregating components in the solution are negligible, and eq 5 may be approximated as

$$\frac{\partial}{\partial t} f_{\mathbf{k},1}(t) = -\Gamma_{11} f_{\mathbf{k},1}(t) + \xi_1(t) N_{0,1} D_1 k^2 s_{\mathbf{k},1}$$

$$\frac{\partial}{\partial t} f_{\mathbf{k},s}(t) = -\Gamma_{s1} f_{\mathbf{k},1}(t) - \Gamma_{ss} f_{\mathbf{k},s}(t) + \xi_s(t) N_{0,s} D_s k^2 s_{\mathbf{k},s} \quad (s = 2 - r) \quad (11)$$

Solving these equations and using eqs 8−10, we finally obtain the total structure factor in the form

$$\hat{S}(k,t) = \sum_{s=1}^{r} \hat{S}_s(k) \exp(-\Gamma_{ss} t) \quad (12)$$

with

$$\hat{S}_1(k) \equiv \frac{D_1 k^2 w_1 \hat{\omega}_1(k)}{\Gamma_{11}} + \sum_{s=2}^{r} \frac{2 D_1 D_s k^4 w_1 w_s M_0 \hat{\omega}_1(k) \hat{\omega}_s(k) \gamma_{1s} c}{(\Gamma_{11} - \Gamma_{ss}) \Gamma_{11}} \quad (13)$$

and

$$\hat{S}_s(k) \equiv \frac{D_s k^2 w_s \hat{\omega}_s(k)}{\Gamma_{ss}} - \frac{2 D_1 D_s k^4 w_1 w_s M_0 \hat{\omega}_1(k) \hat{\omega}_s(k) \gamma_{1s} c}{(\Gamma_{11} - \Gamma_{ss}) \Gamma_{ss}} \quad (s = 2 - r) \quad (14)$$

where $\hat{w}_s(k)$ is the single-particle static structure factor ($\equiv N_{0,s}s_{\mathbf{k},s}{}^2$) of species s, and the decay rates of the nonaggregating and aggregating components are written from eq 7 as

$$\Gamma_{11} = D_1k^2(1 + 2w_1M_0\hat{\omega}_1(k)\gamma_{11}c) \tag{15}$$

and

$$\Gamma_{ss} = D_sk^2(1 + 2w_sM_0\hat{\omega}_s(k)\gamma_{ss}c) \quad (s = 2 - r) \tag{16}$$

Furthermore, if the self-diffusion coefficients D_s of the aggregating components ($s = 2 - r$) are much smaller than D_1 of the nonaggregating component (species 1), we may neglect terms of order of D_s/D_1 ($s = 2 - r$) in $\hat{S}_1(k)$ and $\hat{S}_s(k)$. This approximation yields the following equations:

$$\hat{S}_1(k) \cong \frac{w_1N_{0,1}P_1(k)}{1 + 2w_1M_1\gamma_{11}P_1(k)c} \tag{17}$$

and

$$\hat{S}_s(k) \cong \hat{S}_1(k)\frac{w_sN_{0,s}P_s(k)}{w_1N_{0,1}P_1(k)}[1 + 2w_1M_1(\gamma_{11} - \gamma_{1s})P_1(k)c] \quad (s = 2 - r) \tag{18}$$

where $P_s(k)$ is the particle scattering function ($\equiv \hat{w}_s(k)/N_{0,s}$) and M_1 is the molecular weight of the molecularly dispersed polymer.

Equation 17 contains only quantities of the nonaggregating component 1, and $\hat{S}_1(k)/w_1$ is identical with the static structure factor of the aggregate-free solution at the concentration w_1c, formulated by the generalized Ornstein−Zernike integral equation theory.[7] At zero k, we have

$$\lim_{k\to 0} \hat{S}_1(k) \cong w_1[(M_0/RT)(\partial\Pi/\partial c)]^{-1} \tag{19}$$

Here RT is the gas constant multiplied by the absolute temperature, and $\partial\Pi/\partial c$ is the reciprocal of the osmotic compressibility of *the aggregate-free solution* at the concentration w_1c.

On the other hand, eq 18 includes not only quantities of the aggregating components but also of the nonaggregating one. Summing over all the aggregating components, we obtain

$$\sum_{s=2}^{r}\hat{S}_s(k) \cong \frac{\sum_{s=2}^{r}w_sN_{0,s}P_s(k)[1 + zw_1M_1(\gamma_{11} - \gamma_{1s})P_1(k)c]}{1 + 2w_1M_1\gamma_{11}P_1(k)c} \tag{20}$$

The parameters γ_{1s} in eq 20 make it difficult to extract the information on the aggregating components from static structure factor. However, if the s dependence of the factor $[1 + 2w_1M_1(\gamma_{11} - \gamma_{1s})P_1(k)c]$ is weak enough, we may preaverage γ_{1s} over s in a good approximation to obtain the following equations:

$$[\sum_{s=2}^{r}\hat{S}_s(k)]^{-1} \cong [\sum_{s=2}^{r}\hat{S}_s(0)]^{-1}\left[1 + \frac{1}{3}\langle S^2\rangle_{z,A}k^2 + O(k^4)\right] \tag{21}$$

where $\langle S^2\rangle_{z,A}$ is the z-average mean-square radius of gyration of the aggregating components defined by

$$\langle S^2\rangle_{z,A} \equiv M_{w,A}^{-1}\sum_{s=2}^{r}w_{A,s}M_s\langle S^2\rangle_s \tag{22}$$

with the weight-average molar mass $M_{w,A}$ of aggregates, the weight fraction $w_{A,s}$ of aggregating species s in the total aggregates ($\equiv w_s/\sum_{s=2}^{r}w_s$), and the molar mass M_s and the mean-square radius of gyration $\langle S^2\rangle_s$ of species s. To obtain eq 21, we have neglected the k dependence of $P_1(k)$ for the nonaggregating component, which may be much weaker than those of $P_s(k)$ of the aggregating components. The intercept $[\sum_{s=2}^{r}\hat{S}_s(0)]^{-1}$ includes another important information on aggregates, the degree of aggregation, but the unknown parameters γ_{1s} prevent us from extracting the information.

The first cumulant Γ of the dynamic structure factor is defined by

$$\Gamma \equiv -\lim_{t\to 0}\frac{d}{dt}[\ln \hat{S}(k,t)] \tag{23}$$

The dynamic structure factor given by eq 12 consists of the nonaggregating and aggregating component terms, so that we can define the first cumulants for both components, which are written in the limit of $k \to 0$ as

$$-\lim_{t,k\to 0}\frac{d}{dt}\frac{1}{k^2}\ln[\hat{S}_1(k)\exp(-\Gamma_{11}t)] = \lim_{k\to 0}\frac{\Gamma_{11}}{k^2} = D_1\frac{M_1}{RT}\frac{\partial\Pi}{\partial c} \tag{24}$$

and

$$-\lim_{t,k\to 0}\frac{d}{dt}\frac{1}{k^2}\ln[\sum_{s=2}^{r}\hat{S}_s(k)\exp(-\Gamma_{ss}t)] \equiv \lim_{k\to 0}\frac{\Gamma_{agg}}{k^2} \cong \frac{\sum_{s=2}^{r}w_sN_{0,s}\lim_{k\to 0}\frac{\Gamma_{ss}}{k^2}[1 + 2w_1M_1(\gamma_{11} - \gamma_{1s})c]}{\sum_{s=2}^{r}w_sN_{0,s}[1 + 2w_1M_1(\gamma_{11} - \gamma_{1s})c]} \tag{25}$$

Here, we have used eqs 15, 16, 18, and 19. The right-hand-side quantity in eq 24 is equal to the mutual diffusion coefficient of the aggregate-free solution of the polymer concentration w_1c.[8] As in the case of the static structure factor, the first cumulant Γ_{agg} for the aggregating components (eq 25) contains quantities of the nonaggregating component. Again, applying the preaverage approximation for γ_{1s}, we have

$$\lim_{k\to 0}\frac{\Gamma_{agg}}{k^2} \cong D_{z,A} = \frac{k_BT}{6\pi\eta_0R_{H,A}} \tag{26}$$

where $D_{z,A}$ and $R_{H,A}$ are the z-average diffusion coefficient and the hydrodynamic radius, respectively, and k_B and η_0 are the Boltzmann constant and the zero-shear viscosity of the solution, respectively. $D_{z,A}$ is defined by

$$D_{z,A} \equiv M_{w,A}^{-1}\sum_{s=2}^{r}w_{A,s}M_sD_s \tag{27}$$

Table 1. Molecular Characteristics of PHIC Samples Used (at 25 °C)

sample	$M_w/10^4$	$\langle S^2\rangle^{1/2}$/nm	R_H/nm	M_w/M_n[a]	c/g cm^{-3} [b]
O-2	4.5	16[c]	8.5	1.08	0.047
JP-3-3	6.3	23	11	1.04	0.030
R-2	23.6	56	26	1.1	0.011

[a] Determined by size-exclusion chromatography. [b] Concentration where the temperature-quench experiment was made. [c] Estimated by the Benoit−Doty equation with the persistence length = 43 nm and the molar mass per unit contour length = 730 nm^{-1}.[29]

So far, we have only considered the center-of-mass translational motion of each species, so that $\hat{S}(k,t)$ given by eq 12 does not include effects of rotational or internal motions of polymer chains and aggregates. Assuming that the center-of-mass motion is independent of internal and rotational motions for each component, we may formally include the effect of the latter motions by introducing a new structure factor $\hat{S}_s^{\text{int}}(k,t)$ with respect to the internal and rotational motions for each component:

$$\hat{S}(k,t) = \sum_{s=1}^{r} \hat{S}_s(k)\, \hat{S}_s^{\text{int}}(k,t) \exp(-\Gamma_{ss}t) \qquad (28)$$

For dilute solutions of Gaussian chains and also of rodlike polymers, it can be approximately shown that eq 28 holds and the first cumulant of species s at $k \to 0$ is equal to Γ_{ss}.[9] In the same way, we can show that eqs 24−26 are not affected by the rotational or internal motions of polymer chains and aggregates, which uncorrelate to the center-of-mass motion.

Experimental Section

Samples and Test Solutions. One atactic polystyrene sample and three fractionated PHIC samples were used for light scattering experiments. The polystyrene sample used is a standard sample purchased from Tosoh Co., whose weight-average molecular weight M_w is 10 200 and the ratio of M_w to the number-average molecular weight M_n is 1.02. Details of the preparation of the PHIC samples were described elsewhere.[10] Values of M_w, the radius of gyration $\langle S^2\rangle^{1/2}$, and M_w/M_n of each sample were determined by static light scattering and size exclusion chromatography. Those results are summarized in Table 1. (For sample O-2, $\langle S^2\rangle^{1/2}$ was too small to be determined by light scattering; we have estimated $\langle S^2\rangle^{1/2}$ of this sample by the Benoit−Doty equation.[11]) The values of M_w/M_n indicate narrow molecular weight distribution of all polystyrene and PHIC samples used.

n-Hexane solutions of the PHIC samples were prepared in the same procedure as in the previous work.[12] The test solutions were kept above 30 °C during the preparation process and then quenched at 15 °C for different quench times t_{quench} to make aggregation progress in the solutions. Light scattering measurements were made at different t_{quench} at 15 °C for samples O-2 and R-2 and at 25 °C for sample JP-3-3. It was checked that scattering intensities from the quenched solutions of sample JP-3-3 did not change with raising temperature from 15 to 25 °C.

The polystyrene sample was dissolved in THF to prepare solutions of concentrations $c = 0.27$ and 0.33 g/cm^3. For the solution of $c = 0.27$ g/cm^3, light scattering measurements were made at 25 °C after filtration by a Millipore filter with a pore size of 0.45 μm and centrifugation at 10 000 rpm (12 000g). The solution of $c = 0.33$ g/cm^3 was filtrated through a Millipore filter of the same type, heated below the boiling temperature to gently evaporate the solvent, and centrifuged at 10 000 rpm to use for light scattering measurements at 25 °C at $c = 0.45$ and 0.55 g/cm^3. The aggregation in the THF solution of polystyrene was not sensitive to temperature.

Light Scattering Measurements. Simultaneous static and dynamic light scattering measurements for PHIC and polystyrene solutions were made using an ALV/DLS/SLS-5000 light scattering system equipped by an ALV-5000 multiple τ digital correlator. Vertically polarized light with the wavelength λ_0 of 532 nm emitted from a Nd:YAG laser (model 532, Coherent) was used as the incident light, and the scattered light was measured with no analyzer. The light scattering system was calibrated using toluene as the reference material. The Rayleigh ratio of toluene for vertically polarized 532 nm light without analyzer was taken to be 2.74×10^{-5} cm^{-1} at 25 °C. The monomer-unit static structure factor $\hat{S}(k)$ [$\equiv \hat{S}(k,t)$ at $t = 0$] was calculated from the excess Rayleigh ratio R_θ of the solution over that of the solvent by

$$\hat{S}(k) = \frac{N_A \lambda_0^{\,4}}{4\pi^2 \tilde{n}^2 (\partial\tilde{n}/\partial c)^2} \frac{R_\theta}{cM_0} \qquad (29)$$

where k is the magnitude of the scattering vector, N_A is the Avogadro constant, $\tilde{n}$ is the refractive index of the solution, M_0 is the monomer-unit molecular weight, and $\partial\tilde{n}/\partial c$ is the specific refractive index increment (0.123, 0.127, and 0.195 cm^3/g for PHIC in *n*-hexane at 15 and 25 °C and polystyrene in THF at 25 °C, respectively, at 532 nm).

Dynamic light scattering provides the intensity autocorrelation function $g^{(2)}(t)$, which is in general written as

$$\left[\frac{g^{(2)}(t) - 1}{g^{(2)}(0) - 1}\right]^{1/2} = \frac{\hat{S}(k,t)}{\hat{S}(k)} = \sum_{i=1}^{n} A(\tau_i,k) \exp(-t/\tau_i) \qquad (30)$$

where τ_i and $A(\tau_i,k)$ are the ith relaxation time and its relaxation strength at k, respectively, and the latter is normalized as

$$\sum_{i=1}^{n} A(\tau_i,k) = 1 \qquad (31)$$

The spectrum of $A(\tau_i,k)$ was obtained by the CONTIN analysis with choosing a suitable number n of the relaxation times. In this study, the range of the relaxation time from 0.1 μs to 10 s was divided into 70−150 equal intervals in the logarithmic scale.

Analysis of Light Scattering Data. As will be presented below, $A(\tau_i,k)$ of quenched PHIC solutions and a concentrated polystyrene solution were bimodal, and two first cumulants of the fast relaxation mode (Γ_{fast}) and of the slow relaxation mode (Γ_{slow}) were calculated by[13]

$$\Gamma_{\text{fast}} \equiv -\lim_{t\to 0} \frac{\mathrm{d}}{\mathrm{d}t} \ln\Big[\sum_{i\in\text{fast}} A(\tau_i,k) \exp(-t/\tau_i)\Big] = \sum_{i\in\text{fast}} \tau_i^{-1} A(\tau_i,k) \Big/ \sum_{i\in\text{fast}} A(\tau_i,k) \qquad (32)$$

and

$$\Gamma_{\text{slow}} \equiv -\lim_{t\to 0} \frac{\mathrm{d}}{\mathrm{d}t} \ln\Big[\sum_{i\in\text{slow}} A(\tau_i,k) \exp(-t/\tau_i)\Big] = \sum_{i\in\text{slow}} \tau_i^{-1} A(\tau_i,k) \Big/ \sum_{i\in\text{slow}} A(\tau_i,k) \qquad (33)$$

where the summations are taken over τ_i belonging to each mode. Furthermore, static structure factors for fast and slow relaxation modes were obtained by[13,14]

$$\hat{S}_{\text{fast}}(k) = \hat{S}(k) \sum_{i\in\text{fast}} A(\tau_i,k) \qquad (34)$$

and

$$\hat{S}_{\text{slow}}(k) = \hat{S}(k) \sum_{i \in \text{slow}} A(\tau_i,k) \tag{35}$$

where $\hat{S}(k)$ is the total static structure factor obtained by static light scattering. In what follows, the experimental Γ_{fast}, Γ_{slow}, $\hat{S}_{\text{fast}}(k)$, and $\hat{S}_{\text{slow}}(k)$ are identified with Γ_{11}, Γ_{agg}, $\hat{S}_1(k)$, and $\sum_{s=2}^{r} \hat{S}_s(k)$, respectively, appearing in the Theoretical Section.

Solution Viscosity. The zero-shear viscosity η_0 of the THF solution of the polystyrene sample with $c = 0.55$ g/cm^3 at 25 °C was measured using a capillary viscometer, which needs to estimate $R_{\text{H,A}}$ by eq 26. On the other hand, η_0 of *n*-hexane solutions of PHIC were measured previously at 40 °C.[8] The experimental results for $M_w \leq 3.2 \times 10^5$ were favorably compared with the fuzzy cylinder model theory.[15,16] The same theory was used to estimate η_0 of the three *n*-hexane solutions of PHIC examined by light scattering at 15 °C (for samples O-2 and R-2) or 25 °C (for sample JP-3-3), using the solvent viscosity as well as the wormlike chain parameters at the temperatures [the persistence length = 44 nm (41 nm) and the molar mass per unit contour length = 727 nm^{-1} (730 nm^{-1}) at 15 °C (25 °C).[8]

Results and Discussion

Static and Dynamic Structure Factors. Figure 1 shows static structure factors $\hat{S}(k)$ for *n*-hexane solutions of samples O-2 ($c = 0.047$ g/cm^3), JP-3-3 ($c = 0.030$ g/cm^3), and R-2 ($c = 0.011$ g/cm^3) quenched at 15 °C for different times t_{quench}. With increasing t_{quench}, $\hat{S}(k)^{-1/2}$ gradually decreases for all the solutions. The thick solid line in each Panel indicates theoretical $\hat{S}(k)^{-1/2}$ for the aggregate-free solution calculated by the generalized Ornstein−Zernike integral equation theory[7] (i.e., eq 17 with $w_1 = 1$) with molecular parameters determined previously.[12] Compared with this theoretical line, experimental scattering of quenched solutions is enhanced especially at low angles, indicating the formation of large aggregates or clusters of PHIC chains in the solutions. The aggregation takes place at lower concentrations for higher molecular weight PHIC samples. The solution of sample R-2 contains a small amount of aggregates even before quenched.

Figure 2 shows intensity autocorrelation functions $g^{(2)}(t)$ and their distributions $A(\tau,k)$ of the relaxation time τ for the *n*-hexane solution of sample R-2 quenched for 155 h at four scattering angles θ. The spectra of $A(\tau,k)$ are mostly bimodal, but with increasing θ the peak for the fast relaxation mode becomes broad. The broadening of the fast mode peak was also observed in the same solution before quenched and may come from internal relaxations of this high molecular weight PHIC chain. On the other hand, the peak for the slow mode, being well separated from the fast mode peak, keeps its sharpness even at high θ. However, in the plot of $A(\tau,k)$ vs $k^2\tau$, the peak position of the slow mode shifts to higher $k^2\tau$ with increasing θ, so that this peak cannot be ascribed to purely translationally diffusive relaxation.

Figure 3 compares $A(\tau,k)$ of quenched solutions of three PHIC samples at $\theta = 80°$. We can easily separate $A(\tau,k)$ into the fast and slow relaxation modes for every sample. For the lower molecular weight PHIC samples, peaks of the fast mode are narrower than that of sample R-2, according as the chain internal motion becomes less important. On the other hand, peaks of the slow mode become broader with decreasing the sample molecular weight. Although not shown, the slow-mode peaks of sample O-2 became sharper with decreasing θ.

The enhanced low-angle scattering was also observed in THF solutions of atactic polystyrene at high concentrations, as shown in Figure 4a. Similar light scattering

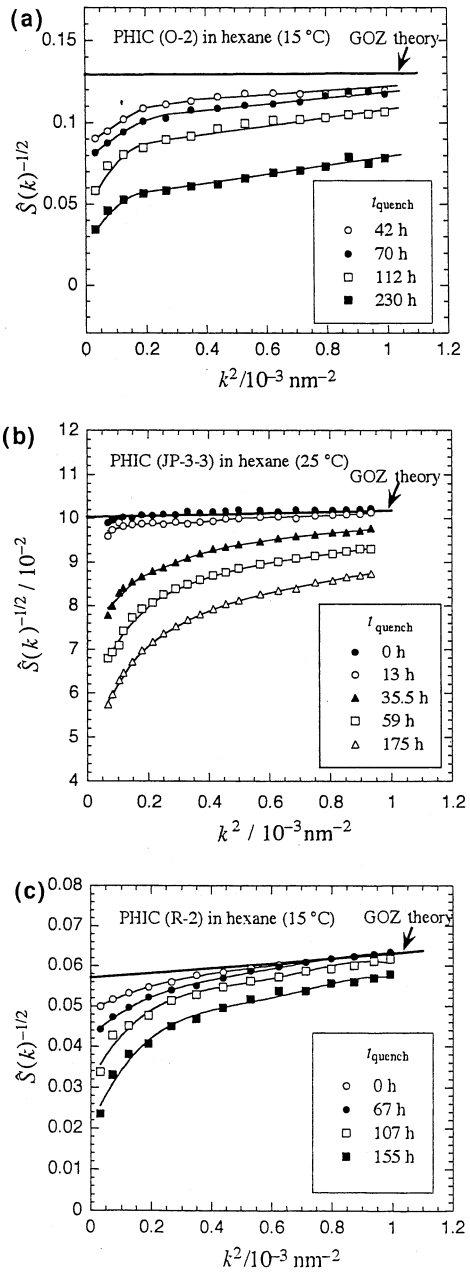

Figure 1. Static structure factor $\hat{S}(k)$ of *n*-hexane solutions of PHIC quenched at 15 °C for different times t_{quench}: (a) sample O-2 ($c = 0.047$ g/cm^3); (b) sample JP-3-3 ($c = 0.030$ g/cm^3); (c) sample R-2 ($c = 0.011$ g/cm^3); GOZ theory, the generalized Ornstein−Zernike integral equation theory (cf. eq 17).[12]

results were reported for atactic polystyrene solutions dissolved in various solvents.[17−20] For the most concentrated solution ($c = 0.55$ g/cm^3), $g^{(2)}(t)$ and $A(\tau,k)$ at $\theta = 40°$ are shown in Figure 4b by unfilled and filled circles, respectively. Fast and slow mode peaks in $A(\tau,k)$ are well separated each other for polystyrene solution, too.

As explained in the Theoretical Section, the conditions, $w_1 \approx 1$ and $D_s \ll D_1$ ($s \geq 2$) are prerequisite to the validity of approximate equations (e.g., eqs 17, 19, 21, 24, and 26). Aggregate-containing solutions shown in Figures 1 and 4 were so transparent that amounts of aggregates in all those solutions are expected to be tiny (i.e., $w_1 \approx 1$). In fact, a sedimentation pattern of an *n*-hexane solution of the PHIC sample JP-3-3 quenched at 15 °C for a long time had no difference from that before quenched. In addition, the position of every

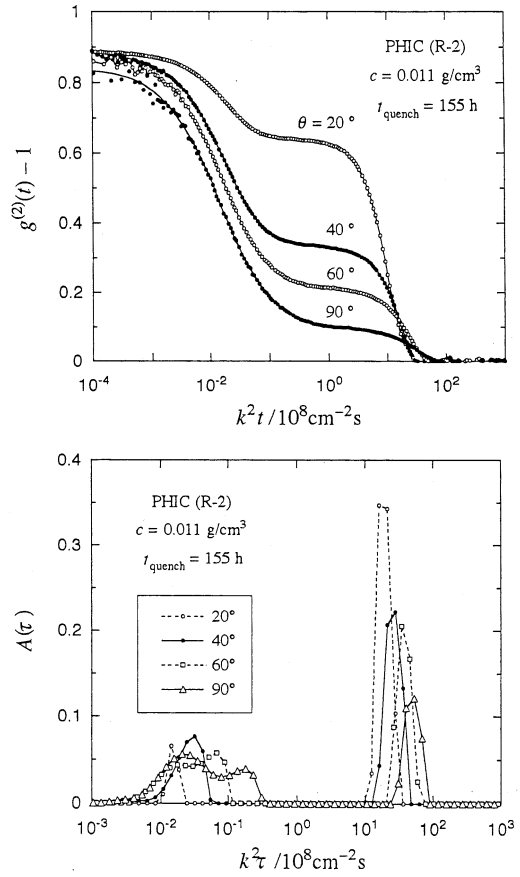

Figure 2. Intensity autocorrelation functions $g^{(2)}(t)$ and their distributions $A(\tau,k)$ of the relaxation time τ for the *n*-hexane solution of sample R-2 quenched for 155 h at four different scattering angles θ.

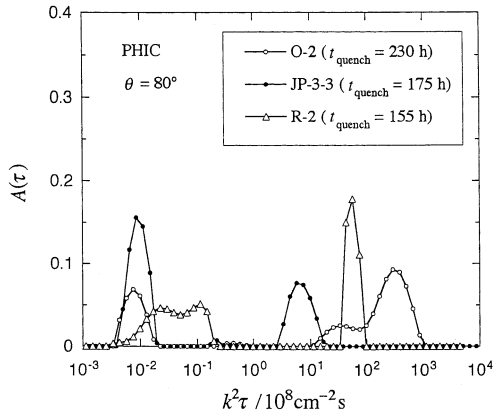

Figure 3. Relaxation strength $A(\tau,k)$ of quenched solutions of three PHIC samples at $\theta = 80°$.

slow-mode peak of $A(\tau,k)$ in Figures 2, 3, and 4 is at τ 3 or 4 orders slower than the fast-mode peak, so that we can expect much smaller diffusion coefficients of aggregating components. In what follows, we apply the above approximate equations to all the aggregate-containing solutions of PHIC and polystyrene.

Fast-Mode Components. From $\hat{S}(k)$ and $A(\tau,k)$ for the aggregate-containing solutions, fast-mode components $S_{fast}(k)$ of the static structure factor were calculated using eq 34. Figure 5 summarizes $\hat{S}_{fast}(k)$ obtained for quenched solutions of the three PHIC samples, where different symbols for each sample indicate data points at different t_{quench}, and the three lines are theoretical $\hat{S}(k)$ for the aggregate-free solution of each

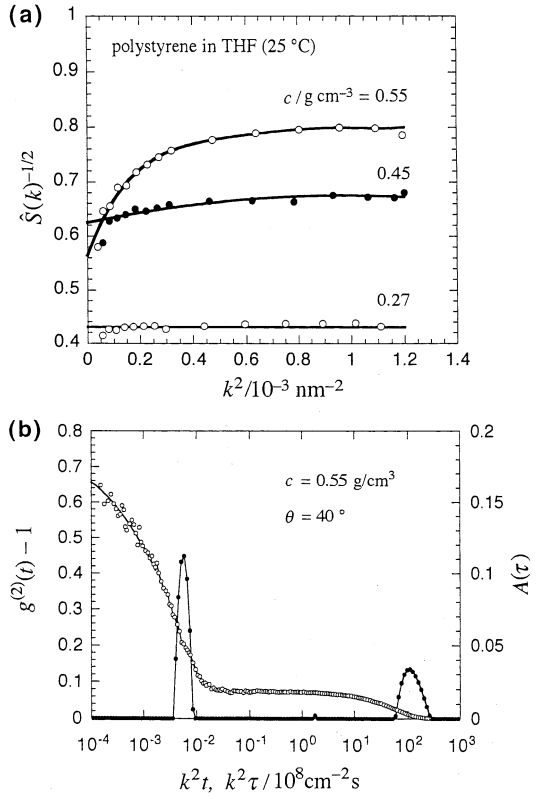

Figure 4. Static and dynamic light scattering results of THF solutions of atactic polystyrene: (a) $\hat{S}(k)$ of three solutions with different concentrations; (b) $g^{(2)}(t)$ (unfilled circles) and $A(\tau,k)$ (filled circles) for the most concentrated solution at $\theta = 40°$.

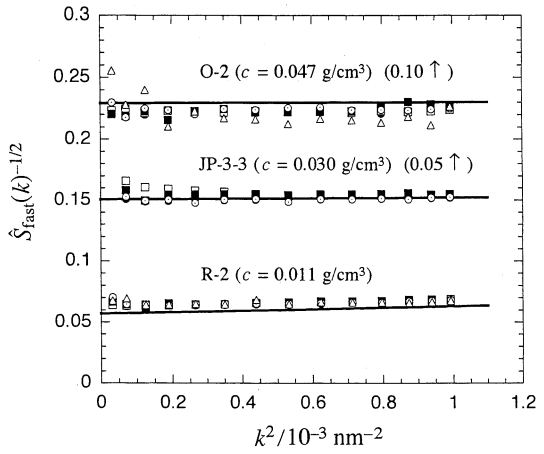

Figure 5. Fast-mode component $\hat{S}_{fast}(k)$ of the static structure factor for quenched solutions of three PHIC samples: different symbols, data points at different t_{quench}; solid lines, the theoretical $\hat{S}(k)$ for the aggregate-free solutions calculated by the generalized Ornstein−Zernike integral equation theory (eq 17).[12]

sample, calculated by eq 17 with $w_1 = 1$ and molecular parameters used previously.[7,12] For every sample, the data points at different t_{quench} almost obey the theoretical line, demonstrating that $S_{fast}(k)$ is equal to the static structure factor of the aggregate-free solution.

On the other hand, fast-mode components Γ_{fast} of the first cumulant, obtained from $A(\tau,k)$ for the aggregates-containing PHIC solutions using eq 32, are shown in Figure 6. Again, for every sample, data points at different t_{quench}, indicated by different symbols, almost obey a single line. In the figure, three arrows indicate theoretical mutual diffusion coefficients

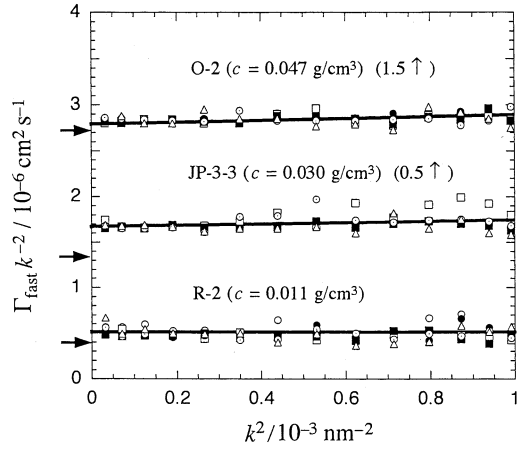

Figure 6. Fast-mode component Γ_{fast} of the first cumulant divided by k^2 for quenched PHIC solutions: different symbols, data points at different t_{quench}; arrows, the theoretical mutual diffusion coefficients for the aggregate-free solutions, calculated on the basis of the fuzzy-cylinder model theory.[8]

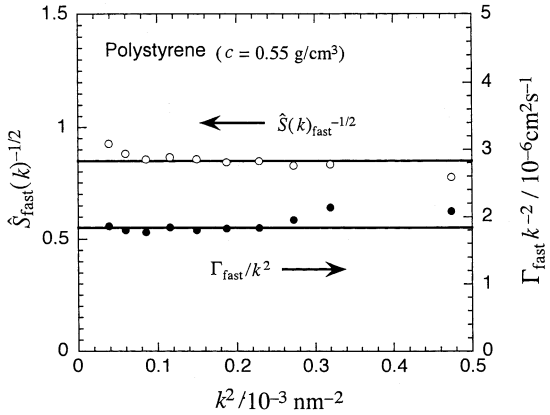

Figure 7. Plots of $\hat{S}_{fast}(k)^{-1/2}$ and Γ_{fast}/k^2 against k^2 for the THF solution of polystyrene (c = 0.55 g/cm³).

[= $D_1(M_1/RT)(\partial\Pi/\partial c)$] for the aggregate-free solution, calculated on the basis of the fuzzy-cylinder model theory[8,15,16] with parameters determined previously from zero-shear viscosity data of the same system.[8] Experimental intercepts of Γ_{fast}/k^2 almost agree with the theoretical values in accordance with eq 24, though the agreement is less satisfactory for sample JP-3-3.

Figure 7 plots $\hat{S}_{fast}(k)^{-1/2}$ and Γ_{fast}/k^2 against k^2 for a THF solution of polystyrene (c = 0.55 g/cm³). Both $\hat{S}_{fast}(k)$ and Γ_{fast}/k^2 are almost independent of k. From the intercept of $\hat{S}_{fast}(k)^{-1/2}$, we have estimated the reciprocal of the osmotic compressibility $\partial\Pi/\partial c$ for the aggregate-free binary solution, and the result agreed with that calculated by the perturbation theory with molecular parameters recently determined for low-molecular-weight polystyrene in toluene,[21] another good solvent.

Slow-Mode Components. Figure 8 shows slow-mode components $\hat{S}_{slow}(k)$ of the static structure factor for PHIC samples O-2 and R-2, obtained from $\hat{S}(k)$ and $A(\tau,k)$ for the quenched solutions using eq 35. The k dependence of $\hat{S}_{slow}(k)^{-1/2}$ for both samples is stronger than that of $\hat{S}_{fast}(k)^{-1/2}$ for the same samples (cf. Figure 5). According to eq 21, we estimated the z-average radius of gyration $\langle S^2\rangle_{z,A}^{1/2}$ of aggregates formed in the quenched solutions, from the plot of $\hat{S}_{slow}(k)^{-1/2}$ vs k^2. The results for three PHIC samples are given in Figure 9. The lower the molecular weight of PHIC sample (or the higher the polymer concentration of quenched

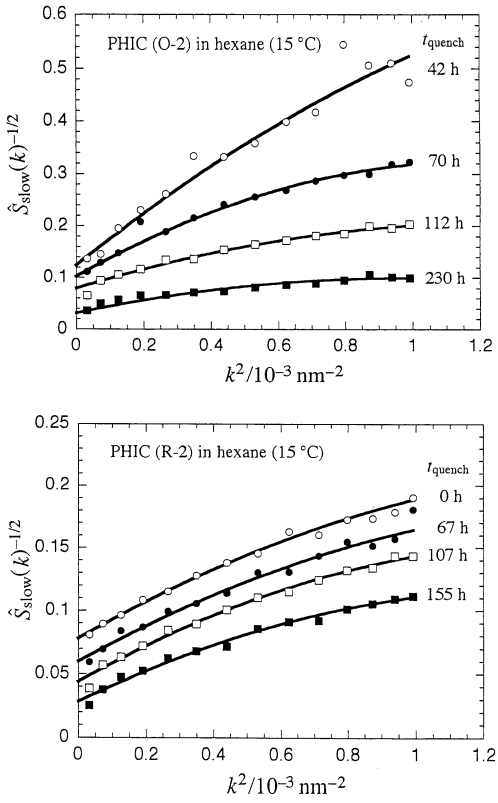

Figure 8. Slow-mode component $\hat{S}_{slow}(k)$ of the static structure factor for quenched solutions of PHIC samples O-2 and R-2 at different t_{quench}.

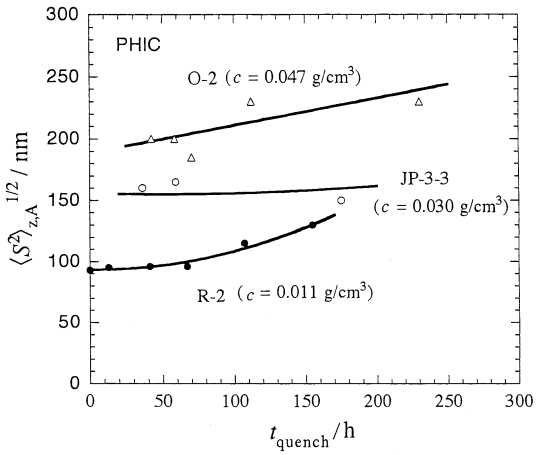

Figure 9. z-Average radius of gyration $\langle S^2\rangle_{z,A}^{1/2}$ of aggregates formed in the quenched solutions of three PHIC samples.

solutions), the larger the aggregates formed. While $\langle S^2\rangle_{z,A}^{1/2}$ is much larger than that of the single chain for sample O-2, it is only about twice for sample R-2 (cf. Table 1). The size of the aggregates almost stays constant or only gradually increases with t_{quench}. The intercept $\hat{S}(0)_{slow}^{-1/2}$ in Figure 8 rather remarkably decreases with t_{quench}. This may indicate that the amount of aggregates increase with t_{quench}. It is however difficult to estimate the weight fraction of aggregates from $\hat{S}_{slow}(0)$, because $\hat{S}_s(0)$ in each s ($2 \le s \le r$) given by eq 18 contains three unknown parameters w_s, $N_{0,s}$, and γ_{1s} together.

The slow-mode component Γ_{slow} of the first cumulant was calculated from $A(\tau,k)$ of each quenched PHIC solution according to eq 33. Figure 10 plots Γ_{slow}/k^2 against k^2 for three PHIC samples at given t_{quench}.

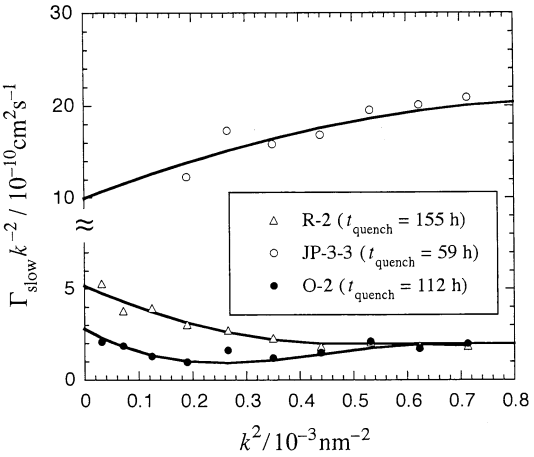

Figure 10. Slow-mode component Γ_{slow} of the first cumulant divided by k^2 for quenched solutions of three PHIC samples.

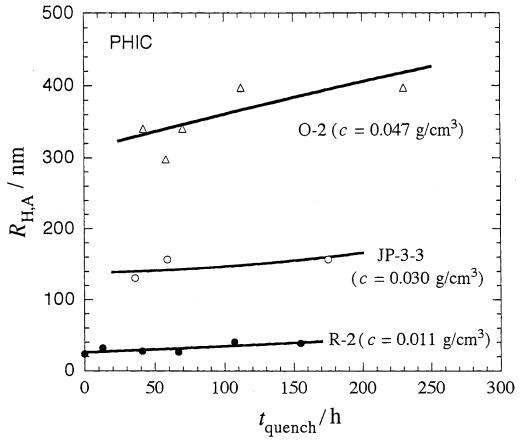

Figure 11. Hydrodynamic radius $R_{H,A}$ of aggregates formed in the quenched solutions of three PHIC samples.

Although data points are slightly scattered, we can see interesting k dependencies of Γ_{slow}/k^2. That is, it increases with k^2 for the middle molecular weight sample JP-3-3 but changes oppositely for the lower and higher molecular weight samples O-2 and R-2 at small k^2. The increase of Γ/k^2 is often observed for high-molecular-weight polymers, due to incorporating faster internal motions into the first cumulant Γ.[22,23] On the other hand, the negative dependence of Γ/k^2 was reported for some stiff-polymer solutions of finite concentrations[8,24] and theoretically explained for rodlike polymer solutions by Doi et al.,[3] who considered the intermolecular correlation of translational and rotational motions of rodlike polymers. Both polymer molecular weight and concentration are different in the three solutions shown in Figure 10, so that intra- and intermolecular correlations of molecular motions may reflect on the first cumulant in a complex way in the three solutions.

Figure 11 shows the t_{quench} dependence of the hydrodynamic radius $R_{H,A}$ of aggregates formed in quenched solutions of three PHIC samples, determined from the intercept of the plot such as shown in Figure 10 using eq 26. Like $\langle S^2\rangle_{z,A}^{1/2}$, $R_{H,A}$ of aggregates formed in the quenched solution is larger for the lower molecular weight PHIC sample, indicating that the aggregates of lower molecular weight PHIC sample consists of larger number of polymer chains.

As explained in the Appendix, $A(\tau,k)$ contains information about polydispersity of scattering species. Figure 12 shows the polydispersity index $I_A(1/2)$ of aggregates formed in three quenched PHIC solutions, defined by

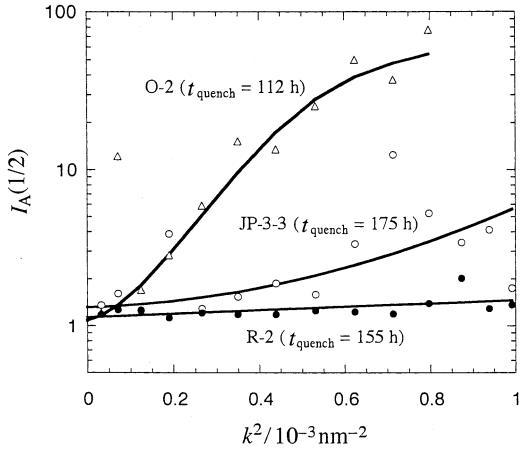

Figure 12. Polydispersity index $I_A(1/2)$ of aggregates formed in three quenched PHIC solutions, which was calculated from $A(\tau,k)$ using eq 36.

$$I_A(1/2) \equiv \frac{[\sum_{i\in\text{slow}} A(\tau_i,k)\tau_i^{2}][\sum_{i\in\text{slow}} A(\tau_i,k)\tau_i^{-2}]}{[\sum_{i\in\text{slow}} A(\tau_i,k)]^2} \quad (36)$$

Although data points for sample O-2 and JP-3-3 are considerably scattered, which may be owing to the disturbance of the CONTIN analysis by noise, $I_A(1/2)$ seems to approach to a number not far from unity in the limit of zero k^2 for every solution. At $k^2 = 0$, $I_A(1/2)$ becomes identical with $I_0(1/2)$ for aggregates given by eq A4 in the Appendix with $\nu_D = 1/2$, and if the power-law exponent ν_D of the diffusion coefficient D is $1/2$, it should be equal to the ratio M_z/M_w of the z-average to weight-average molecular weight for aggregates (see Appendix).

However, if the molecular weight dependence of D is weaker, the intercept $I_0(1/2)$ is no longer equal to M_z/M_w. As a special case, if D is independent of the molecular weight, the intercept is always unity for any polydispersity. PHIC chains in solution may nonspecifically interact each other, so that there is no reason for narrow distributions in the degree of aggregation. Thus, the intercepts of $I_A(1/2)$ in Figure 12 do not indicate the narrow distribution of PHIC aggregates but a weak dependence of D on the degree of aggregation.

It is known that the ratio ρ of the radius of gyration to the hydrodynamic radius is a parameter characteristic of the shape of the scattering object.[25] While $\rho = 0.775$ for a sphere with a uniform density, it increases with increasing the axial ratio of the object but decreases with increasing the density of the sphere in the central part. Flexible linear chains take values of ρ from 1.2 to 1.5, but ρ of stiff polymer chains exceeds 2 (cf. Table 1). Figure 13 shows the ratio ρ_A for PHIC aggregates formed in quenched solutions of the three PHIC samples as functions of t_{quench}, which was estimated by eq A5 in the Appendix. This equation includes the polydispersity correction, but the correction factor was not far from unity for every solution, due to a weak dependence of D on the degree of aggregation.

In Figure 13, the ratio ρ_A of the aggregate of the high-molecular-weight sample R-2 is comparable to ρ of the isolated chain (cf. Table 1), which indicates that the

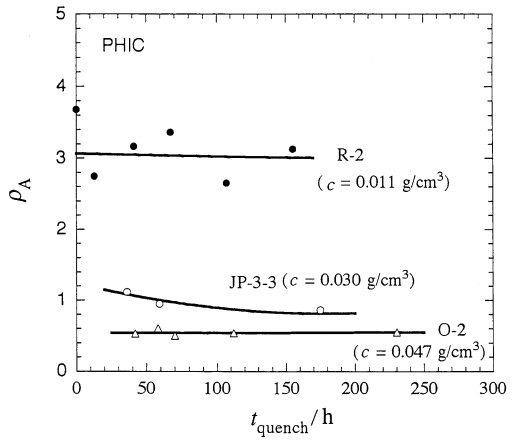

Figure 13. Ratio ρ_A of the radius of gyration to the hydrodynamic radius for PHIC aggregates formed in three quenched solutions as functions of t_{quench}.

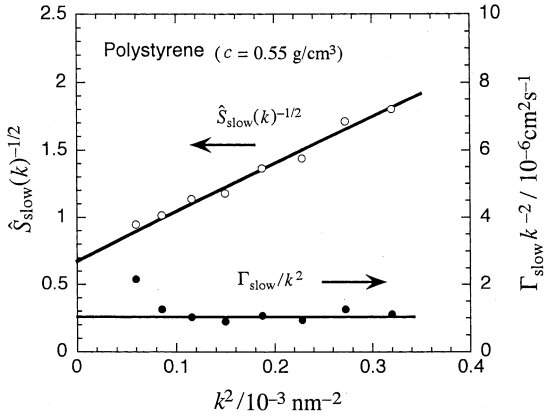

Figure 14. k^2 dependencies of $\hat{S}_{slow}(k)^{-1/2}$ and Γ_{slow}/k^2 for the THF solution of polystyrene with $c = 0.55$ g/cm^3.

conformation of the aggregate looks rigid-chain-like and PHIC chains arrange nearly side-by-side with rare branching in the aggregate. This may be consistent with fibrous gel structures observed by Guenet et al.[26] formed in quenched *n*-octane solutions of a PHIC sample with a similar molecular weight (2.83×10^5) by electron microscopy. On the other hand, ρ_A of the aggregate of the lower-molecular-weight sample O-2, formed at a high polymer concentration ($c = 0.047$ g/cm^3), is much smaller than ρ of the isolated chain. This implies that the aggregate of this sample is highly branched to form a spherical particle of highly crowded polymer chains. The high polymer concentration may be responsible for this random aggregation. For samples R-2 and O-2, ρ_A is almost independent of t_{quench}, but that of sample JP-3-3 slightly decreases from a random-coil value to the value for sample O-2 with increasing t_{quench}.

Figure 14 shows the k^2 dependencies of $\hat{S}_{slow}(k)^{-1/2}$ and Γ_{slow}/k^2 for the THF solution of polystyrene with $c = 0.55$ g/cm^3, obtained from the light scattering data shown in Figure 4. Just in the same method as used for PHIC aggregates, we have estimated $\langle S^2\rangle_{z,A}^{1/2}$, $R_{H,A}$, and ρ_A of the polystyrene aggregates to be 160 nm, 110 nm, and 1.4_5, respectively. The last value is approximately equal to ρ of the isolated chain and indicates that polystyrene chains are bound together rather loosely in the aggregate. The polydispersity index $I_A(1/2)$ is very close to unity at $k^2 = 0$, indicating a weak dependence of D on the degree of aggregation for the polystyrene aggregate, too.

The origin of the binding force among PHIC and atactic polystyrene chains in aggregates is still in dispute, but possible candidates are the van der Waals force, dipole−dipole interaction, solvent-mediated complexation, and so on. In a remarkable contrast with the strong intermolecular attraction in aggregates, the attractive interaction of the nonaggregating component coexisting in the solution is very weak as indicated by the osmotic compressibility of aggregate-free solutions.[12,21] This contrast tempts us to assume that the polymer chain takes different local conformation or orientation in aggregates and in the isolated state. Kobayashi et al.[27] found highly ordered TTGG conformations in syndiotactic polystyrene gels by infrared spectroscopy and implied that the conformations were stabilized by solvation. On the other hand, Green et al.[28] reported abrupt changes in circular dichroism of PHIC containing small amounts of optically active isocyanate comonomers in *n*-hexane and *n*-octane, upon gelation, ascribing the changes to local parallel alignment of the chains. However, the evidence is not so decisive that we need more study on the origin of the binding force in polymer aggregates.

Appendix. On the Polydispersity

The intensity autocorrelation function $g^{(2)}(t)$ obtained by dynamic light scattering is written as

$$\lim_{k,c\to 0}\left[\frac{g^{(2)}(t)-1}{g^{(2)}(0)-1}\right]^{1/2} = M_w^{-1}\sum_i M_i w_i \exp(-D_i k^2 t) \quad \text{(A1)}$$

in the limits of zero k (the magnitude of the scattering vector) and c (the polymer concentration). Here, M_i, w_i, and D_i are the molar mass, weight fraction, and diffusion coefficient of the scattering component i in the solution, respectively. By the inverse Laplace transform analysis, experimental $g^{(2)}(t)$ can be decomposed into multiexponential functions:

$$\lim_{k,c\to 0}\left[\frac{g^{(2)}(t)-1}{g^{(2)}(0)-1}\right]^{1/2} \equiv \sum_i A_0(\tau_{0,i},k)\exp(-t/\tau_{0,i}) \quad \text{(A2)}$$

where $\tau_{0,i}$ and $A_0(\tau_{0,i},k)$ are the relaxation time of the mode i and its strength, respectively, and the subscript 0 indicates the values extrapolated to the zero k and c. Comparing eqs A1 and A2, we have the relations

$$\tau_{0,i}^{-1} = D_i k^2 \quad \text{and} \quad A_0(\tau_{0,i},k) = M_w^{-1} M_i w_i \quad \text{(A3)}$$

If the diffusion coefficient has a power-law dependence on the molar mass, i.e., $D_i \propto M_i^{-\nu_D}$ with a constant exponent ν_D, we can determine the ratio M_z/M_w of the z-average to weight-average molecular weight from the polydispersity index $I_0(\nu_D)$ defined by

$$I_0(\nu_D) \equiv \frac{[\sum_i A_0(\tau_{0,i},k)\tau_{0,i}^{1/\nu_D}][\sum_i A_0(\tau_{0,i},k)\tau_{0,i}^{-1/\nu_D}]}{[\sum_i A_0(\tau_{0,i},k)]^2} = \frac{M_z}{M_w} \quad \text{(A4)}$$

For Gaussian chains, $\nu_D = {}^1/_2$, so that $I_0({}^1/_2)$ gives M_z/M_w.

If the ratio ρ of the radius of gyration $\langle S^2\rangle_i^{1/2}$ to the hydrodynamic radius $R_{H,i}$ is independent of i or the

molar mass of the component, it can be estimated from the z-average diffusion coefficient D_z and radius of gyration $\langle S^2\rangle_z^{1/2}$ (cf. eqs 22 and 27) by the equation

$$\rho = \frac{6\pi\eta_0}{k_B T} D_z \langle S^2\rangle_z^{1/2} \frac{[\sum_i A_0(\tau_{0,i},k)]^{3/2}}{[\sum_i \tau_{0,i}{}^2 A_0(\tau_{0,i},k)]^{1/2}[\sum_i \tau_{0,i}{}^{-1} A_0(\tau_{0,i},k)]} \quad \text{(A5)}$$

The last fraction is the correction factor with respect to the polydispersity.

References and Notes

(1) Liu, S.; Hu, T.; Liang, H.; Jiang, M.; Wu, C. *Macromolecules* **2000**, *33*, 8640.
(2) Kataoka, K.; Harada, A.; Nagasaki; Y. *Adv. Drug Deliv. Rev.* **2001**, *47*, 113.
(3) Doi, M.; Shimada, T.; Okano, K. *J. Chem. Phys.* **1988**, *88*, 4070.
(4) Doi, M.; Edwards, S. F. *The Theory of Polymer Dynamics*; Clarendon Press: Oxford, 1986.
(5) Yamakawa, H. *Modern Theory of Polymer Solutions*; Harper & Row: New York, 1971.
(6) In the original theory of the second virial coefficient, β_{su} is independent of the polymer concentration, but to include effects of the higher virial terms, the quantity γ_{su} should be identified with the apparent second virial coefficient Γ_{su} in ref 30, which is concentration-dependent. (One should not confuse Γ_{su} with the decay rate given by eq 6.) Furthermore, Γ_{su} in ref 30 are independent of s and u, if all species consist of identical monomer units, but γ_{su} may depend on the interacting species due to the multiple-contact effect on γ_{su} being neglected in ref 30.
(7) Sato, T.; Jinbo, Y.; Teramoto, A. *Polym. J.* **1995**, *27*, 384.
(8) Ohshima, A.; Yamagata, A.; Sato, T.; Teramoto, A. *Macromolecules* **1999**, *32*, 8645.
(9) Berne, B. J.; Pecora, R. *Dynamic Light Scattering*; John Wiley & Sons: New York, 1976.
(10) Ohshima, A.; Kudo, H.; Sato, T.; Teramoto, A. *Macromolecules* **1995**, *28*, 6095.
(11) Murakami, H.; Norisuye, T.; Fujita, H. *Macromolecules* **1980**, *13*, 345.
(12) Jinbo, Y.; Teranuma, O.; Kanao, M.; Sato, T.; Teramoto, A. *Macromolecules* **2003**, *36*, 198.
(13) Because of noise in $g^{(2)}(t)$, small separated peaks sometimes appear between the main fast and slow peaks in $A(\tau_i,k)$. We have omitted those artificial peaks to calculate Γ_{fast}, Γ_{slow}, $\hat{S}_{fast}(k)$, and $\hat{S}_{slow}(k)$. In such a case, $A(\tau_i,k)$) in eq 31 has been renormalized.
(14) The separation of the static structure factor into the fast- and slow-mode components using the relaxation time spectrum from dynamic light scattering was made previously for other polymer solution systems,[31] though their physical meanings were not clarified theoretically.
(15) Sato, T.; Takada, Y.; Teramoto, A. *Macromolecules* **1991**, *24*, 6220.
(16) Sato, T.; Teramoto, A. *Adv. Polym. Sci.* **1996**, *126*, 85.
(17) Guenet, J.-M.; Willmott, N. F. F.; Ellsmore, P. A. *Polym. Commun.* **1983**, *24*, 230.
(18) Koberstein, J. T.; Picot, C.; Benoit, H. *Polymer* **1985**, *26*, 673.
(19) Gan, J. Y.; François, J.; Guenet, J.-M. *Macromolecules* **1986**, *19*, 173.
(20) Heckmeier, M.; Strobl, G. *Macromolecules* **1997**, *30*, 4454.
(21) Koyama, R.; Sato, T. *Macromolecules* **2002**, *35*, 2235.
(22) Schaefer, D. W.; Han, C. C. In *Dynamic Light Scattering*; Pecora, R., Ed.; Plenum Press: New York, 1985.
(23) Kubota, K.; Chu, B. *Macromolecules* **1983**, *16*, 105.
(24) DeLong, L. M.; Russo, P. S. *Macromolecules* **1991**, *24*, 6139.
(25) Yamakawa, H. *Helical Wormlike Chains in Polymer Solutions*; Springer-Verlag: Berlin, 1997.
(26) Guenet, J.-M.; Jeon, H. S.; Khatri, C.; Jha, S. K.; Balsara, N. P.; Green, M. M.; Brulet, A.; Thierry, A. *Macromolecules* **1997**, *30*, 4590.
(27) Kobayashi, M.; Nakaoki, T.; Ishihara, N. *Macromolecules* **1990**, *23*, 78.
(28) Green, M. M.; Khatri, C. A.; Reidy, M. P.; Levon, K. *Macromolecules* **1993**, *26*, 4723.
(29) Norisuye, T.; Tsuboi, A.; Teramoto, A. *Polym. J.* **1996**, *28*, 357.
(30) Sato, T.; Jinbo, Y.; Teramoto, A. *Polym. J.* **1999**, *31*, 285.
(31) Sedlak, M. *J. Chem. Phys.* **1996**, *105*, 10123.

MA0213899